AIP | The Journal of Chemical Physics

A systematic study of spirals and spiral turbulence in a reaction-diffusion system

Hongyu Guo, Liang Li, Qi Ouyang, Jian Liu, and Zhensu She

Citation: The Journal of Chemical Physics **118**, 5038 (2003); doi: 10.1063/1.1554397
View online: http://dx.doi.org/10.1063/1.1554397
View Table of Contents: http://scitation.aip.org/content/aip/journal/jcp/118/11?ver=pdfcov
Published by the AIP Publishing

JOURNAL OF CHEMICAL PHYSICS VOLUME 118, NUMBER 11 15 MARCH 2003

A systematic study of spirals and spiral turbulence in a reaction-diffusion system

Hongyu Guo, Liang Li, and Qi Ouyang[a)]
Department of Physics, State Key Laboratory for Mesoscopic Physics, Peking University, Beijing, 100871, China

Jian Liu
Department of Mechanics and Engineering Science, State Key Laboratory for Studies of Turbulence and Complex Systems, Peking University, 100871, China

Zhensu She
Department of Mechanics and Engineering Science, State Key Laboratory for Studies of Turbulence and Complex Systems, Peking University, 100871, China and Department of Mathematics, University of California, Los Angeles, Los Angeles, California 90095

(Received 11 September 2002; accepted 31 December 2002)

We report our experimental study on chemical patterns in a spatial open reactor using the Belousov–Zhabotinsky reaction. A phase diagram showing different regimes of spiral dynamics is presented. The focus of the study is on transitions leading to defect-mediated turbulence (spiral turbulence). Some new interesting phenomena are described, including a transition from one type of spiral turbulence to another type, and the re-entry from spiral turbulence into ordered spiral waves. We also try to characterize different states of turbulence using the hierarchical structure theory.
 [DOI: 10.1063/1.1554397]

I. INTRODUCTION

During the past 30 years, spiral patterns are always considered as one of the most intriguing spatiotemporal structures in macroscopic systems driven far from thermodynamic equilibrium, and the study of spiral dynamics has attracted a great deal of attention from researchers in different fields, such as nonlinear physics, mathematics, physical chemistry, biology, and cardiology. There are several reasons for these attractions. The first reason is that spiral patterns are ubiquitous in different systems, including reaction-diffusion media,[1,2] aggregating slime mold cells,[3] cardiac muscle tissue,[4–6] and intracellular calcium release.[7] Second, as we have known, a spiral is self-organized by a topological defect, which constructs the spiral core and plays the role of dominator.[1,8] So the study of spiral behavior might give hints about the defect dynamics. One important aspect in this research field is studying transitions from ordered spiral patterns to defect-mediated turbulence. Several spiral instabilities leading to defect-mediated turbulence or spiral turbulence have been well studied in theory,[9–12] and observed both in experiments[13–17] and numerical simulation.[18–20] Study of such instabilities is one of the most favorable routes to investigate spatiotemporal chaos, which is poorly understood at present. From an application point of view, the result of this study has a promising application potential in cardiology, as transitions from spiral to spiral turbulence occur in heart tissue and play an essential role in cardiac arrhythmia and fibrillation.[4,6]

Experimental investigations using the Belousov–Zhabotinsky (BZ) reaction have provided plentiful information about spiral dynamics. For example, we know that a spiral can be supported in excitable or oscillatory media, both of which can be obtained in the BZ reaction.[1,8,22] Sections of phase diagrams using different control parameters have been sketched to identify different regimes of spiral dynamics.[21,22] Transitions from regular spiral patterns to defect-mediated turbulence have also been studied carefully with the BZ reaction, and two important instabilities, the Doppler instability[16,22] and the long wavelength instability,[13,17,22] have been found. The Doppler instability occurs in an excitable system, corresponding to regions where the control parameter $\Delta \equiv [H_2SO_4][NaBrO_3]$ is low. In such a parameter space, spiral patterns are trigger waves, which are governed by a dispersion relation that relates the speed to the period of traveling waves. There exists a minimum period below which the system cannot recover to its excitable state, and traveling waves cease to exist.[23] Usually, the period of regular spiral waves is larger than the minimum period, thus spiral waves are stable. However, when a Hopf bifurcation contributes to the spiral core and makes the spiral tip meandering, the trajectory of the spiral tip changes from a single circle to a flower. When the meandering speed is sufficiently large, due to the Doppler effect, two adjacent wave fronts near the core are so close that the local wavelength is beyond the critical value, causing a spontaneous generation of defects.[16]

If the control parameter $\Delta \equiv [H_2SO_4][NaBrO_3]$ is higher than 0.2 M^2, the ferroin ($Fe(phen)_3^{2+}$) catalyzed BZ reaction can be considered as an oscillatory system and the existing spiral is phase wave. Near the onset, the system's local variable (c), such as the concentration of ferroin, can be written as $c = c_0 + A \exp(i\varpi_c t) + \text{c.c.}$, where ϖ_c is the Hopf fre-

[a)]Electronic mail: qi@phy.pku.edu.cn

quency. Suppose the system is near a supercritical Hopf bifurcation, the complex amplitude A obeys the complex Ginzburg–Laudau equation (CGLE),

$$\tau_0 \frac{\partial A}{\partial t} = \mu A + (g_1 + i g_2) \frac{\partial^2 A}{\partial r^2} - \xi_0^2 (d_1 + i d_2) |A|^2 A, \qquad (1)$$

where τ_0 and ξ_0 are, respectively, the characteristic time and the correlation length of the system, g_1, g_2, d_1, and d_2 are related to the diffusion coefficients and ensemble of reaction kinetics. After rescaling, using τ_0 and ξ_0 as time and space units, we have

$$\frac{\partial A}{\partial t} = A + (1 + i c_1) \frac{\partial^2 A}{\partial r^2} - (1 + i c_3) |A|^2 A, \qquad (2)$$

where $c_1 = d_2/d_1$ and $c_3 = g_2/g_1$ are control parameters. In the one-dimensional case, Eq. (2) has traveling wave solutions $A_0 = F \exp[i(kx - \varpi t)]$, where $F^2 = 1 - k^2$ and $\varpi = c_1 k^2 + c_3(1 - k^2)$. Stability analyses[24] show that, under certain conditions, the system will be unstable against long wavelength perturbations. After the instability occurs, sustained long-wavelength modulated waves emerge. The long wavelength instability has a convective nature, which explains the existence of stable modulated waves in a finite space while the system has been unstable. In the two-dimensional case, the instability usually induces a meadering movement of spiral tips; the frequency of meadering movement determines the wavelength of the modulation.[22] Due to the convective nature, this modulative perturbation travels downstream as it amplifies, leaving ordered modulated spiral waves. The fundamental difference between long-wavelength modulated spiral waves and meandering spirals is that the former has a nonzero convective velocity,[17,22] while the latter is zero. When the control parameter is increased to across a threshold, spiral waves break and defects generate far away from the spiral center, as a result of two neighboring wave fronts being too close. At last, when the control parameter is further increased, absolute instability occurs and defect-mediated turbulence invades the whole space.[13,17,22]

Despite fruitful results of previous researches, some problems have not been clarified and certain parameter space deep into turbulence regimes has not been explored. In this paper, after describing the experimental setup in the following section, we present our systematic studies of dynamical behaviors of spiral waves and spiral turbulence. A phase diagram with the feeding concentrations of sulfuric acid and malonic acid as control parameters is built, and the lines of onset for each transition are identified. Several new phenomena are described, including a transition between two types of spiral turbulence and the re-entry of spirals from spiral turbulence. In Sec. IV, we introduce a method, the hierarchical structure theory (HST),[25] to characterize the states of spiral turbulence. We show that a phase transition between two types of spiral turbulence can be identified using this method. In Sec. V, we give a discussion on the new discovered phenomena.

II. EXPERIMENTAL SETUP

Our experiments are conducted in a spatial open reactor using the ferroin ($Fe(phen)_3^{2+}$) catalyzed BZ reaction. The heart of our reactor is a thin porous glass disk (0.4 mm thick and 20 mm in diameter). The glass disk has 25% void space and 100 Å average pore size, so that it can be considered as a homogeneous medium for a macroscopic pattern with a character length scale of a few hundred micrometers. The porous glass prevents convection when used as the reaction medium. Each side of the disk is contacted by a reservoir where the reactants are continuously refreshed by highly precise chemical pumps (Pharmacia P-500) and kept homogeneous by stirring. The chemicals are fed to both reservoirs separately so that we can keep one (A) in the reduced state of the reaction system, and the other (B) in the oxidized state. When the reactants diffuse into the porous glass and meet there, pattern-forming reactions take place and spatiotemporal patterns form. The chemical patterns are monitored in transmitted light (halogen light filtrated to wavelength less than 550 nm) with a charge coupled device (CCD) camera. The signal received by the CCD camera is sent to a computer where images are digitized and saved for further quantitative analysis.

We choose the concentration of malonic acid in reservoir A ($[CH_2(COOH)_2]^A$ or $[MA]^A$) and sulfuric acid in reservoir B ($[H_2SO_4]^B$) as the control parameters, which are adjustable in a range of 0.3–1.0 M and 0.4–1.6 M, respectively. Other conditions are kept fixed during the whole experiment: $[NaBrO_3]^{A,B} = 0.4$ M; $[KBr]^A = 0.03$ M; $[ferroin]^B = 1.0$ mM. The resident time in each reservoir is 10^3 s; the ambient temperature is $25 \pm 0.5\,°C$. Since there are multiple concentration gradients across the reaction medium, the observed pattern is quasi-three-dimensional, and an instability in the gradient direction may happen. In this study, we focus on spiral patterns which are stable in the gradient direction, so that patterns are entrained in this direction.[26] As a result, the observed patterns can be considered as quasi-two-dimensional most of the time. Under certain conditions, the three-dimensional effect does exist and might be the cause of some new phenomena. We will give discussions later.

The initial condition of the experiment is that there is only one spiral tip residing in the middle of the reaction medium. This condition can be achieved by using a helium–neon laser (3 mW, $\lambda = 633$ nm) to generate and guide spiral tips. In a regime of stable spiral (see phase diagram of Fig. 1), after suitable reactant solutions are pumped into reservoirs, a train of traveling waves automatically appears from the boundary of the reaction medium. We use a beam of laser light to break a chemical wave front and create a couple of defects, which develop into a pair of counter-rotating spiral waves. Then we use laser light to lead one spiral tip to the edge of the reactor and delete it, and drive the other one to the center of the reaction medium. Once a spiral is ready, we study it by changing one reactant concentration stepwise while fixing all other conditions. A record is taken after the pattern relaxes into its asymptotic state and no laser is applied for a sufficient amount of time (around an hour).

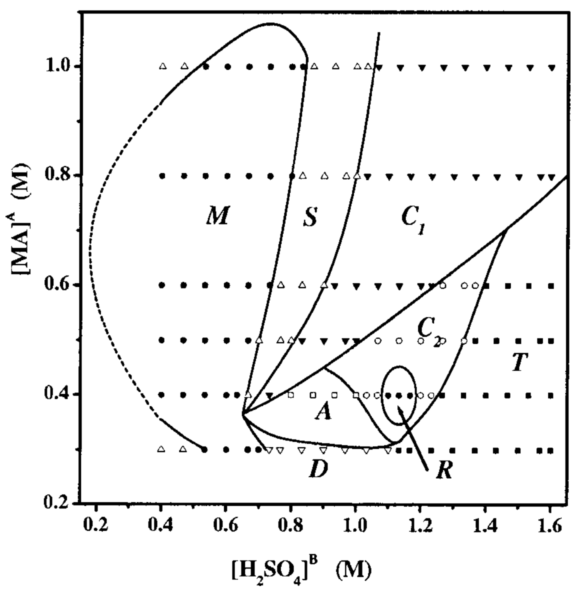

FIG. 1. The phase diagram with $[MA]^A$ and $[H_2SO_4]^B$ as the control parameters. The solid lines indicate the onsets of different instabilities. The dashed lines are the extrapolation of the solid lines.

III. EXPERIMENTAL RESULTS

Some previous studies[27] point out that the dynamics of spiral patterns is most sensitive to three parameters: the concentration of malonic acid ([MA]), the concentration of sulfuric acid ($[H_2SO_4]$), and the concentration of sodium bromate ($[NaBrO_3]$). Others provide the phase diagrams which use $[H_2SO_4]$ and [MA] as control parameters and divide different domains according to different observed patterns.[21,22] However, there is still a certain parameter space that has not been reached. This work explores a part of the unexplored parameter space, and especially pays attention to the phenomena occurring at high $[H_2SO_4]$. Some new phenomena are found, including a transition between two types of spiral turbulence and the re-entry of stable spirals from a state of spatiotemporal chaos.

Figure 1 shows the phase diagram using $[H_2SO_4]^B$ and $[MA]^A$ as the control parameters. More than 200 points in the phase diagram are studied, and eight different dynamics regimes are categorized. They are marked using different capital letters: (1) Simple spiral (S), where the system is either in an excitable or an oscillating medium, the period, wavelength, and speed of the spiral waves are constant, as shown in Fig. 2(a). (2) Meandering spiral (M), where the system is in an excitable medium and the movement of spiral tip follows a hypocycloid or epicycloid trajectory instead of a simple cycle. Due to the Doppler effect, both the local period and the local wavelength change as a function of time. The modulation forms a superspiral, as shown in Fig. 2(b). (3) Spiral turbulence due to the Doppler instability (D), where the minimum of local period goes beyond the critical value, making traveling waves unstable. An example of such a state is shown in Fig. 2(c). (4) Modulated spirals due to the long wavelength instability, (C_1). Figure 2(d) gives such an example. Here, the system is in an oscillatory medium instead of an excitable medium. (5) A state of coexistence of modulated spirals and spiral turbulence (C_2). Because of the convective nature of the long wavelength instability, perturbations generated in the spiral core area travel out as they grow, this makes a finite region around the spiral core where traveling waves are asymptotically stable.[13,17] Figure 2(e) gives an example of such state. (6) Defect-mediated turbulence due to the long wavelength instability (T), as shown in Fig. 2(f). (7) A newly observed chemical turbulence (A), and (8) stable spiral due to the reentry of spiral (R). The details of the last two states will be described later in this section, and examples of such states are presented in Figs. 2(g) and 2(h).

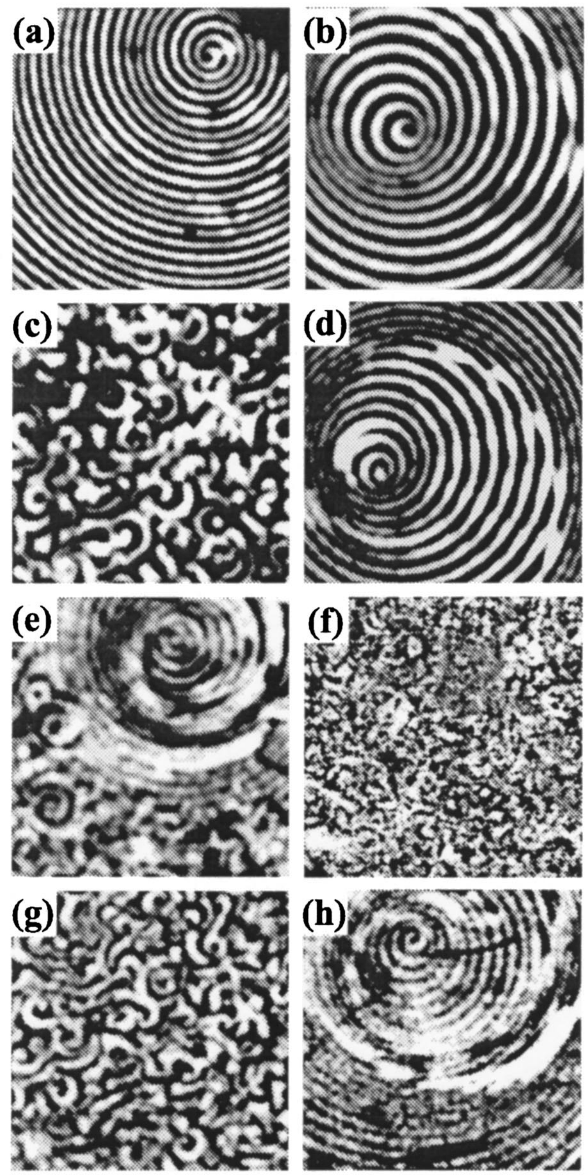

FIG. 2. Examples of different patterns observed in the experiment. (a) Simple rotating spiral (S); (b) meandering spiral (M); (c) a state of spiral turbulence due to the Doppler instability (D); (d) modulated spiral due to the long wavelength instability (C_1); (e) coexistence of a modulated spiral and spiral turbulence; (f) a state of chemical turbulence due to the long wavelength instability (T); (g) a state of spiral turbulence in region A; (h) stable spiral in region R.

Each of the boundaries that separate different regimes

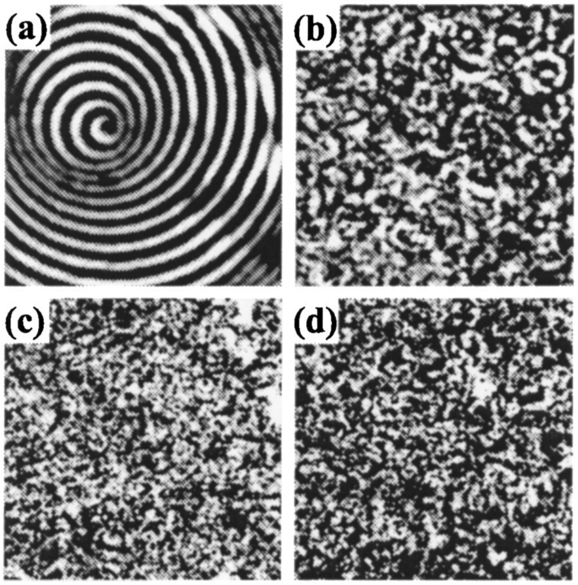

FIG. 3. Images illustrating transitions from meandering spiral to D type spiral turbulence and to T type spiral turbulence with $[\mathrm{MA}]^{\mathrm{A}}=0.3$ M. The values of $[\mathrm{H_2SO_4}]^{\mathrm{B}}$ is in (a) 0.733 M, (M); in (b) 1.100 M, (D); in (c) 1.133 M, near the critical point; and in (d), 1.200 M, (T).

defines a transition. Some transitions have been carefully studied in former works. For example, S–M boundary defines the onset where the spiral tip movement undergoes a Hopf bifurcation. As a result, the trajectory of the tip changes from a simple circle to an epicycloid or a hypocycloid, leading the spiral into the meandering state;[21] M–D line gives the onset of the Doppler instability;[16] and S–C_1, C_1–C_2, and C_2–T lines represent, respectively, the onset of the long wavelength instability, the beginning of spiral wave break up, and transition to full spiral turbulence (absolute instability).[13,17,22] These transitions have been comprehensively understood. Besides these transitions, there are several notable new phenomena shown in the phase diagram: the D–T boundary, the C_1–A boundary, and an isolated R region. In the following, we will describe these transitions in detail.

Notice that the D and T regions are defect-mediated turbulence due to different instability mechanisms; one is due to the Doppler instability[16,22] while the other experiences the long wavelength instability.[13,17,22] A new transition from D to T is discovered along the line $[\mathrm{MA}]^{\mathrm{A}}=0.3$ M. Figure 3 gives examples of patterns in different states [(a), (b), (d)] and patterns near the critical point [(c)]. We notice in the experiments that the turbulence states in D and T regimes are different in time scale and length scale, indicating that there is a transition between the two states. In the following section, we will use the HST to identify this transition.

Another phenomenon that we find is a new regime of spiral turbulence (A) located in a region between C_1 and C_2, as shown in Fig. 1. Besides, an isolated island of stable spiral inside the domain of C_2 appears. These phenomena are very robust; we repeated the experiments several times and found the same behaviors. We also used another piece of glass disk, which has little difference in diffusion coefficient, and similar phenomena were observed, too. In the experiments, We

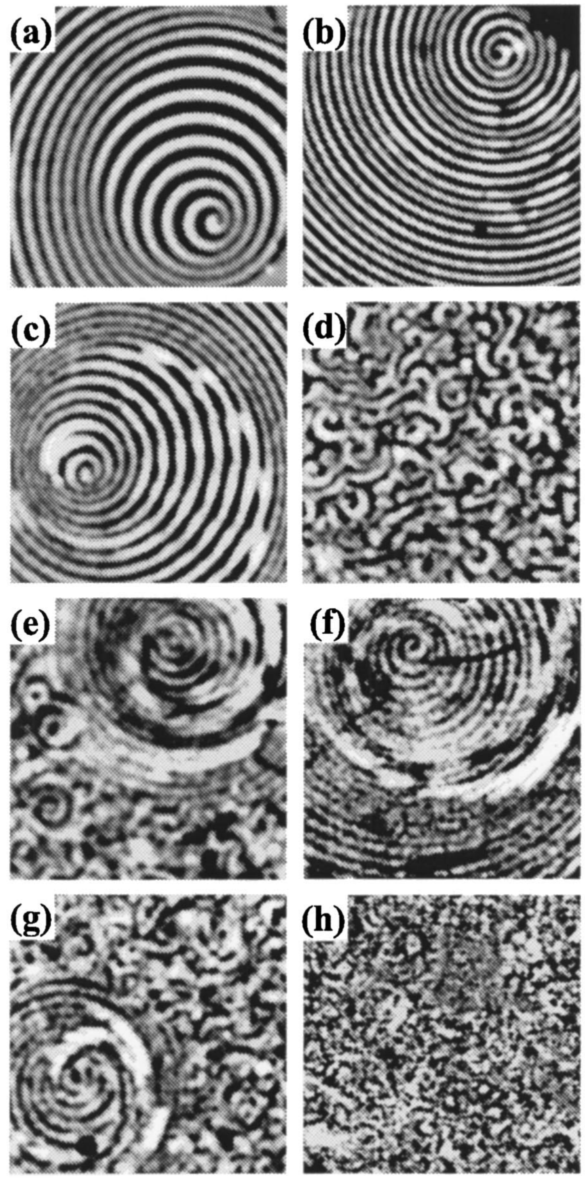

FIG. 4. Images illustrating different patterns observed with $[\mathrm{MA}]^{\mathrm{A}}=0.4$ M. The value $[\mathrm{H_2SO_4}]^{\mathrm{B}}$ is in (a) 0.400 M, (M); in (b) 0.633 M, (S); in (c) 0.767 M, (C_1); in (d) 0.967 M, (A); in (e) 1.067 M, (C_2); in (f) 1.133 M, (R); in (g) 1.200 M, (C_2); and in (h) 1.267 M, (T).

fixed $[\mathrm{MA}]^{\mathrm{A}}$ at 0.4 M and increased $[\mathrm{H_2SO_4}]^{\mathrm{B}}$ stepwisely. The system behaved normally in the low $[\mathrm{H_2SO_4}]^{\mathrm{B}}$ region: As the increase of the control parameter, we observed meandering spirals at $[\mathrm{H_2SO_4}]^{\mathrm{B}}=0.4$ M, [Fig. 4(a)], a transition to simple spirals at $[\mathrm{H_2SO_4}]^{\mathrm{B}}=0.633$ M [Fig. 4(b)], another transition to a state of long wavelength modulated spirals at $[\mathrm{H_2SO_4}]^{\mathrm{B}}=0.767$ M [Fig. 4(c)]. Then a new scenario took place: As the control parameter was further increased, the spiral broke up rapidly, and the entire system plunged into a regime of spiral turbulence without experiencing the C_2 state, as shown in Fig. 4(d). Without fully understanding this behavior, we name this regime A to distinguish it from other states of turbulence, such as D and T. When $[\mathrm{H_2SO_4}]^{\mathrm{B}}$ was increased again, a local region of stable spiral grew up, and the system entered into the C_2 regime [see Fig. 4(e)]. The spiral gradually took up the whole domain of the reaction medium, driving the defects sea out of the boundary [Fig. 4(f)], and we thus experienced a re-entry of the spiral (R regime). When the $[H_2SO_4]^B$ reached a high enough value, defects appeared far away from the spiral center, and the core of stable waves was invaded by the sea of defects little by little again. Finally, the system got across the C_2-T boundary and spiral turbulence dominated the whole domain. The newly observed phenomena appear in a relatively narrow range of control parameters. As shown in the phase diagram of Fig. 1, the system behaves differently for $[MA]^A = 0.5$ M and $[MA]^A = 0.3$ M.

Our experimental observations also indicate some typical critical phenomena near the onset, such as large fluctuations and critical slowing down. In the experiment, once we change the control parameter, the system needs a certain period of time to relax into its newly established asymptotic state. Generally 1 h is enough. But if the system approaches the critical points, one needs to wait 2 or more hours in order for the system to relax to its final state, otherwise one will observe pseudohysteresis when changing back and forth the control parameter. Large fluctuations are also observed near the onset. This phenomenon is especially pronounced near the $A-C_2$ boundary in the A region. In this regime, large spiral patterns may spontaneously self-organize in the sea of turbulence, and will disappear very slowly as we hold on the same experimental conditions for a long time (a few hours). We also notice a new feature of spiral patterns in the R region. As shown in Fig. 4(f), the amplitude of spiral waves is not homogeneous in the R region; we observe a large bright filament pattern, which self-organizes into a large spiral, stretching out from the original spiral center and rotating around it. Moreover, the brightness of this pattern oscillates as a function of time: it is very bright at one time, then slowly gets dark along with its rotation, then becomes bright again in a cycle.

IV. QUANTITATIVE ANALYSIS OF SPIRAL TURBULENCE

As discussed in the previous section and shown in Fig. 3, we notice that the turbulence state from the Doppler instability (D) and that from the long wavelength instability (T) are different in time scale and length scale, and the patterns change abruptly when the control parameter varies across the D–T boundary, indicating that there is a new transition. In this section, we report that the HST (Ref. 25) should be a proper candidate to distinguish the two states of spiral turbulence and to describe spatiotemporal chaos.

In our case, the data that we can quantitatively analyze are images gained from experiments. The magnitude of fluctuations depends on the diversity of the image intensity in the data series. In hydrodynamics, the basic field in turbulence is the velocity from which the local energy dissipation can be defined. A natural candidate for a variable analog to the local energy dissipation is a quantity which takes its largest contributions from the places where large changes in contrast occur.[28] We thus choose the variable $G(f(x,y))$ defined as below to study

$$G(f(x,y)) = \left[\left(\frac{\partial f}{\partial x} \right)^2 + \left(\frac{\partial f}{\partial y} \right)^2 \right]^{1/2}, \tag{3}$$

where $f(x,y)$ is the field of image intensity. Then we investigate the behavior of contrast changes at a scale ℓ by means of a bidimensional integral,

$$\varepsilon(\ell) = \frac{1}{\ell^2} \int_x^{x+\ell} \int_y^{y+\ell} G(f(x,y))\, dx\, dy. \tag{4}$$

We study the static properties of $\varepsilon(\ell)$ of images taken in 256×256 pixels, and characterize the field $\varepsilon(\ell)$ by structure function $S_p(\ell) = \langle |\varepsilon(\ell)|^p \rangle$. The hierarchical structure model introduces a hierarchy of functions $\varepsilon_p(\ell) = S_{p+1}(\ell)/S_p(\ell)$, each describing more closely the intensity of fluctuations. $\varepsilon_p(\ell)$ is associated with higher intensity fluctuations with increasing p. She and Leveque[25] used the hypotheses that an invariant relation exists between ε_p and ε_{p+1}, which is referred to as a hierarchical symmetry relation (a symmetry with respect to a translation in p),

$$\varepsilon_{p+1}(\ell) = A_p \varepsilon_p(\ell)^\beta \varepsilon_\infty(\ell)^{1-\beta}, \quad 0 < \beta < 1, \tag{5}$$

where A_p is independent on ℓ and $\varepsilon_\infty(\ell) = \lim_{p \to \infty} \varepsilon_p(\ell)$, which characterize the most intermitted structures. The term $\varepsilon_\infty(\ell)^{1-\beta}$ can be eliminated and the hierarchical symmetry relation becomes

$$\frac{\varepsilon_{p+1}(\ell)}{\varepsilon_2(\ell)} = \frac{A_p}{A_1} \left(\frac{\varepsilon_p(\ell)}{\varepsilon_1(\ell)} \right)^\beta. \tag{6}$$

From a log–log plot of $\varepsilon_{p+1}(\ell)/\varepsilon_2(\ell)$ vs $\varepsilon_p(\ell)/\varepsilon_1(\ell)$, we can examine the linearity. The value of β is the slope of the line. In Fig. 5 we show the calculation result of the values of β for patterns of spiral turbulence at four separate control parameters $[H_2SO_4]^B$.

The parameter β measures the degree of intermittency of a turbulent flow. In the limit $\beta \to 1$, there is no intermittency. The Kolmogorov's picture of turbulence[29] belongs to this limit. In contrast, in the limit $\beta \to 0$, only the most intermittent structures persist; this is the ordered limit. One example in this category is the black and white β model,[30] where only one type of structure (white) is responsible for the energy dissipation and system disorder. In Fig. 5, one observes that β at $[H_2SO_4]^B = 0.800$ M and 1.100 M is larger than $[H_2SO_4]^B = 1.200$ M and 1.600 M. Figure 6 gives a transition diagram, the change of β as a function of $[H_2SO_4]^B$. It shows that the measured value of β has a decreasing tendency, and the values of β in regime D are higher than in regime T. At the onset ($[H_2SO_4]^B = 1.133$ M), the value of β has a sudden decrease. We thus suggest that the HST can be a suitable candidate in describing different states of spiral turbulence obtained in a reaction-diffusion system.

Another measurement of defect-mediated turbulence is the density of defects. In Fig. 3, we qualitatively realize that the defect density of spiral turbulence in the T region is higher than in the D region. At the critical point, it has a sharp change. So the density of defects can also identify the new transition and the result is consistent with the HST analysis. However, getting the exact number of defects from noisy experimental data in a highly turbulent regime is not easy at least, so that in our case the HST has a clear advan-

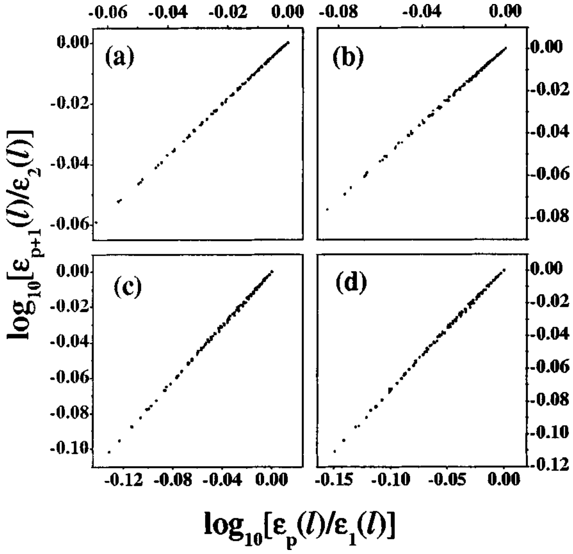

FIG. 5. The hierarchical symmetry relations obtained using images with four different values of $[H_2SO_4]^B$. Each set of points is fitted by a straight line, the slope is the value of β. (a) 0.800 M, $\beta=0.935\,17$; (b) 1.100 M, $\beta=0.8901$; (c) 1.200 M, $\beta=0.772\,46$; and (d) 1.600 M, $\beta=0.738\,04$. The other control parameter is $[MA]^A=0.3$ M.

tage in analyzing experimental data. In the HST, the higher value of β means lower intermittency or lower singularity, so that the value of β of a system describes the degree of order; we say that a system with smaller β has more order. From regime D to regime T, the degree of singularity enhances so that the density of defects increases. The saturation of defects in regime T is remarkably larger than that in regime D. With a sufficiently large saturation of defects, interaction of defects makes the fluctuation weaker, so the system will become more "*order*."

It should be stressed that HST has an invariance (symmetry) which defines a transformation group;[31] this symmetry can be exactly simulated by a log-Poisson cascade process,[32,33] so the model is also called the "log-Poisson" model. When we do multiscaling and hierarchical analysis, some transformations or symmetry can be useful to clarify the complexity of a system. We think that these quantitative properties are useful and revelatory to characterize defect-mediated turbulence and some other spatially extended systems, and further research should be done. The detailed and deep discussion of the use of HST in spatially extended systems will be reported elsewhere.

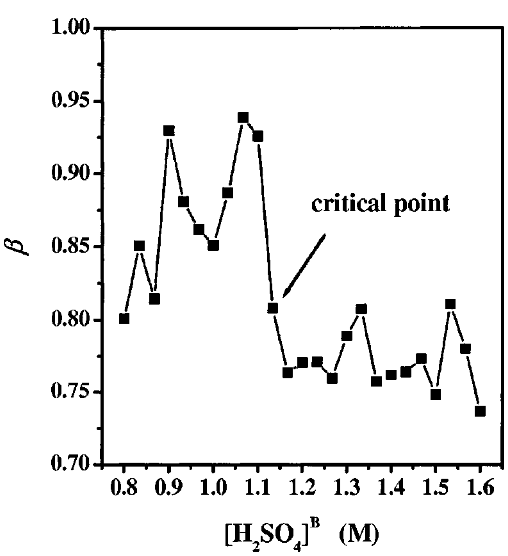

FIG. 6. The change of mean value of β as a function of $[H_2SO_4]^B$ in the range from 0.800 to 1.600 M. The value of β in regime D is larger than that in regime T. There exists a phase transition point at $[H_2SO_4]^B=1.133$ M.

V. DISCUSSIONS

This work revealed three new phenomena: transition from the D type of spiral turbulence to the T type turbulence on the D–T boundary; transition from spiral to spiral turbulence on the S–A boundary; and the re-entry of spiral from a state of defect-mediated turbulence on the A–C_2 boundary (Fig. 1). Transition between two types of turbulent states could be related to the change of the system between an excitable medium and an oscillatory medium. As discussed in the Introduction, although both types of spiral turbulence belong to defect-mediated turbulence, one is due to the Doppler instability (meandering) which takes place in an excitable medium, the other is related to the long wavelength instability, which occurs in an oscillatory medium that is near a supercritical Hopf bifurcation, and becomes dominating after absolute instability occurs. We also know that as the increase of $[H_2SO_4]^B$, the chemical system changes from excitable to oscillatory. Since the correlation length scale for a pattern in an excitable medium is determined by diffusion of chemical species, while the correlation length scale for a pattern in an oscillatory medium is governed by phase diffusion, when the system changes from excitable to oscillatory, the correlation length of the turbulent pattern changes suddenly. This is verified both by experimental observations (see Fig. 3) and quantitative analysis (see Fig. 6).

The chaotic state in region A (see Fig. 1) belongs to defect mediated turbulence. It is similar to the spiral turbulence in region D. However, the route to the state of spiral turbulence is different from either the Doppler instability or the long wavelength instability. It is mix of both. In this scenario, the defects generate far from the spiral core, just like the long wavelength instability, but the transition from modulated spiral to turbulence is fast, similar to the Doppler instability. In the phase diagram, it is clear that region A located between region M and region C_2, where both meandering and long-wavelength instability cannot be ignored. So, region A should be the result of the combination of both instabilities. Besides, in this region the system tends to form ordered spirals from the sea of defects. Away from the A–C_2 boundary, this tendency is suppressed by the defects. With the increase of $[H_2SO_4]^B$, a stable spiral coexists with the defects sea; finally, the newly formed stable spiral drives all the defects out of the boundary and takes up the whole reaction medium. We thus witness the re-entry of spirals. However, due to the finite reactor size, we do not know whether the reentry spirals is stable in extended space or just stable for a finite space and as a long-lived transient. The same trend is also observed in the C_2 region with $[MA]^A=0.5$ M; the difference is that no stable spiral can win. At present, we do not have a satisfactory explanation of this experimental result. The most possible explanation is a codimension effect. One notices in the phase diagram of Fig. 1 that region A is near the point where all the transition lines join together. In this codimensional area the mechanisms of spiral instability may mix together, a new route to spiral turbulence may appear, and new patterns may form. Due to the limit precision of control in the experiments, at present we cannot study the dynamical behavior in this area in detail.

Another phenomenon worth discussing is the bright patterns in Fig. 2(h), which have a markedly long wavelength and an oscillation in brightness. In fact such bright waves exist in a wider parameter space. We think the three-dimensional effect is the most possible reason for such a super wave, but we have no reasonable explanation for the oscillation now. As mentioned in Sec. II, despite the reaction medium can be considered as quasi-two-dimensional most of time, the three-dimensional effect exists and might play an important role in spiral dynamics. The bright patterns in Fig. 2(h) could be the result of two spirals superimposed in the gradient direction.

In summary, we did a systematic experimental study of spiral behaviors in a reaction-diffusion system using the BZ reaction and observed certain new phenomena. Transition from the D type spiral turbulence to the T type turbulence on the D–T boundary can be readily explained by the change of the BZ reaction from excitable to oscillatory. A well established method, the hierarchical structure theory can be applied to identify this transition. Transition from spiral to spiral turbulence on the S–A boundary and the re-entry of spiral on the A–C_2 boundary may be caused by the codimension effect, although more evidence is needed. In order to get a full picture of such dynamics and an appropriate explanation of such phenomena, more careful experimental research, numerical simulation, and theoretic analysis should be done in the future.

ACKNOWLEDGMENTS

The authors thank S. F. Bai and Y. Li for computer programming, W. D. Su, L. We, H. L. Wang, and L. Q. Zhou for fruitful discussions, and H. L. Swinney for providing us with the porous glass. This work is supported by the National Natural Science Foundation of China.

[1] *Chemical Waves and Patterns*, edited by R. Kapral and K. Showalter (Kluwer Academic, Dordrecht, 1995), Part One.
[2] V. Hakim and A. Karma, Phys. Rev. E **60**, 5073 (1999).
[3] K. J. Lee, E. C. Cox, and R. E. Goldstein, Phys. Rev. Lett. **76**, 1174 (1996).
[4] A. T. Winfree, Science **266**, 1003 (1994).
[5] R. A. Gray, A. M. Pertsov, and J. Jalife, Nature (London) **392**, 75 (1998).
[6] F. X. Witkowski, L. J. Leon, P. A. Penkoske, W. R. Giles, M. L. Spano, W. L. Ditto, and A. T. Winfree, Nature (London) **392**, 78 (1998).
[7] J. Lechleiter, S. Girard, E. Peralta, and D. Clapham, Science **252**, 123 (1991).
[8] M. C. Cross and P. C. Hohenburg, Rev. Mod. Phys. **65**, 851 (1993).
[9] P. Coullet, L. Gil, and J. Lega, Phys. Rev. Lett. **62**, 1619 (1989).
[10] J.-P. Eckmann and I. Procaccia, Phys. Rev. Lett. **66**, 891 (1991).
[11] I. Aranson, L. Kramer, and A. Weber, Phys. Rev. Lett. **72**, 2316 (1994).
[12] M. Ipsen and P. G. Sørensen, Phys. Rev. Lett. **84**, 2389 (2000).
[13] Q. Ouyang and J. M. Flesselles, Nature (London) **379**, 143 (1996).
[14] A. L. Belmonte, J. M. Flesselles, and Q. Ouyang, Europhys. Lett. **35**, 665 (1996).
[15] J. S. Park and K. J. Lee, Phys. Rev. Lett. **83**, 5393 (1999).
[16] Q. Ouyang, H. L. Swinney, and G. Li, Phys. Rev. Lett. **84**, 1047 (2000).
[17] L. Q. Zhou and Q. Ouyang, Phys. Rev. Lett. **85**, 1650 (2000).
[18] M. Bär and M. Eiswirth, Phys. Rev. E **48**, R1635 (1993).
[19] M. Bär and M. Or-Guil, Phys. Rev. Lett. **82**, 1160 (1999).
[20] A. Goryachev, H. Chaté, and R. Kapral, Phys. Rev. Lett. **83**, 1878 (1999).
[21] G. Li, Q. Ouyang, V. Petrov, and H. L. Swinney, Phys. Rev. Lett. **77**, 2105 (1996).
[22] L. Q. Zhou and Q. Ouyang, J. Phys. Chem. A **105**, 112 (2001).
[23] J. P. Kneener and J. J. Tyson, Physica D **21**, 307 (1986).
[24] A. Weber, L. Kramer, I. S. Aranson, and L. Aranson, Physica D **61**, 279 (1992).
[25] Z. S. She and E. Leveque, Phys. Rev. Lett. **72**, 336 (1994).
[26] D. Winston, M. Arora, J. Maselko, V. Gáspár, and K. Showalter, Nature (London) **351**, 132 (1991).
[27] A. L. Belmonte, Q. Ouyang, and J. M. Flesselles, J. Phys. II **7**, 1425 (1997).
[28] A. Turiel, G. Mato, N. Parga, and J.-P. Nadal, Phys. Rev. Lett. **80**, 1098 (1998).
[29] A. N. Kolmogorov, C. R. Acad. Sci. URSS **30**, 301 (1941).
[30] U. Frisch, M. Nelkin, and P. L. Sulem, J. Fluid Mech. **87**, 719 (1978).
[31] Z. S. She, Prog. Theor. Phys. **130**, 87 (1998).
[32] B. Dubrulle, Phys. Rev. Lett. **73**, 959 (1994).
[33] Z. S. She and E. C. Waymire, Phys. Rev. Lett. **74**, 262 (1995).